An approach to estimate tidal dissipation with single-point high-frequency ground wave radar data

MAO Hua-bin, CHEN Ju, QIU Chun-hua, LIAN Shu-min

State Key Laboratory of Tropical Oceanography, South China Sea institute of Oceanology, CAS, Guangzhou 510301, Guangdong province, China

Abstract: Using the single-point ground wave (GW) radar data at Shensi Station and the water level data at three stations (Shengsi, Luchaogang and Daishan), the authors obtained the flow vectors from the radial velocity of GW radar observation, and calculate four sub-tidal harmonic constants (O_1, K_1, M_2 and S_2). The tidal characteristics derived from the GW radar dataset agreed well with those from the tidal gauge data. The authors also analyzed the tidal energy flux and tidal energy dissipation rate. There was a good relationship between the tidal energy dissipation rate and topography. The study showed a good way to calculate tidal energy dissipation rate using GW radar data.

Keywords: ground wave radar; characteristic value; tide type; tidal energy flux; tidal energy dissipation

Introduction

Ground wave (GW) radar with high-frequency radar wave is one of the marine environment remote sensing techniques. Since GW radar has relative high frequency electromagnetic waves and sea water conducts electric very well, the diffraction from GW radar achieves to the sea surface much farther than stadia, in a way of vertical polarization. High-frequency GW (HFGW) radar can measure the near-surface current, wind and wave.

Compared with the traditional equipments, this approach covers longer and wider range, observing more parameters and working under all-weather condition; compared with ocean satellite, it has lower expense, higher accuracy and higher spatial/temporal resolution. Therefore, GW radar deserves our attentions. Previous studies on the GW radar lead development of the GW radar ocean remote sensing [1,2]. In 1990s, GW radar reaches a relative high level in terms of techniques and capabilities with the improvement of electric, signal procession and computer. Nowadays, there are tens of GW radars along the coastal area. The flow data retrieved from GW radar will be used widely in the near

Received on May 16, 2012

Corresponding author: maohuabin@scsio.ac.cn

future.

Zhou and Yang[3] retrieved the ocean surface velocity vectors by using two radial velocity maps measured by both radars. They interpolated the radial velocities into the common grids in the polar coordinates and their results were consistent with altimetry results. Zhu et al.[4] calculated the radial velocity using OSMAR GW radar, finding that the spatial distributions of M_2 sub-tidal amplitude and phase were similar with those from former studies.

Internal wave generated from continental shelf not only plays a very important role in the energy balance of global ocean but also provides energy to the local oceanic mixing [5]. Nash et al.[6] observed the internal tidal propagation, reflection and internal wave mixing off Virginia during May and June 1998. They found that at semidiurnal frequency, a divergence of high-wavenumber offshore energy flux almost balanced onshore energy flux.

Zhang et al.[7] calculated the M_2 sub-tidal energy flux in the complicated topography area of Pacific, using 10-year altimetry data, Levitus data and dynamic model data. Li et al.[8] investigated the tidal energy flux and tidal energy dissipation in Bohai Sea, Yellow sea and East China Sea, by assimilating altimetry and tidal gauge data.

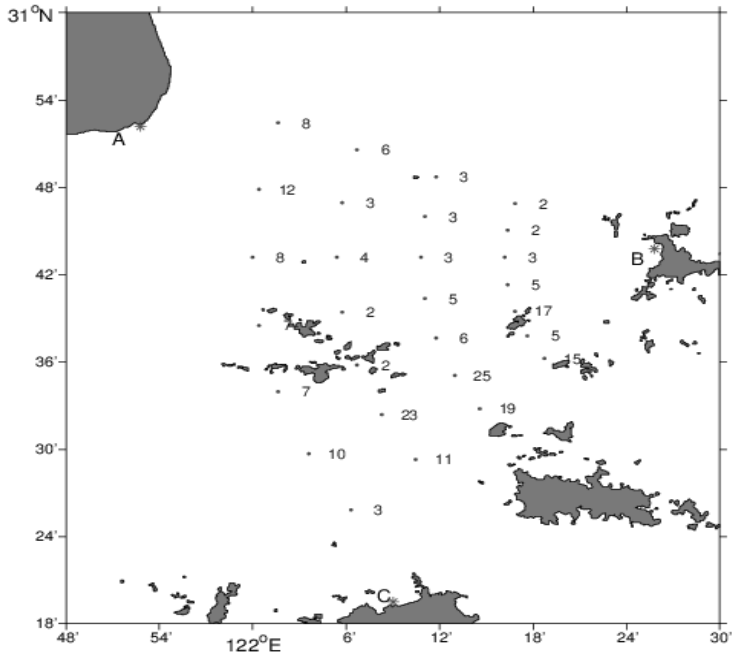

Fig. 1 Observation stations

(The number denotes the water depths, and A, B and C denote the Luchaogang , Shengsi , and Daishan stations, respectively).

In this study, we made a try to derive tidal energy flux and tidal energy dissipation from GW radar data. Firstly, we retrieved the velocity vectors based on the GW radar data in Shengsi Island, Hangzhou Bay. Secondly, we approached the velocity and the delay angle of M_2 sub-tide and S_2 sub-tide, and finally we got the tidal energy flux and tidal energy dissipation. Data and methods are discussed below; section 2 explains the results and section shows is the discussion and conclusions.

2 Data and methods

2.1 Data

Radial velocities were derived from HFGW radar measurements at Shengsi Island (Fig. 1). It covered 120°-120°30′E, 30°24′-30°54′N from Aug. 23 to Sep. 26, 2007. The temporal was 389s, the radial was 10 km, and the angle resolution was 10°, respectively. We also compare the tide gauge data with 1h resolution at Luchao, Shengsi and Daishan stations. The topography data from chart are interpolated.

2.2 Methods

2.2.1 Current vectors

The GW radar only measures the radial velocity. The real tidal velocity vector includes not only the radial velocity but also the tangential velocity. It is inaccurate to get the tidal energy balance only using radial velocity. Therefore, we need to retrieve the velocity vectors.

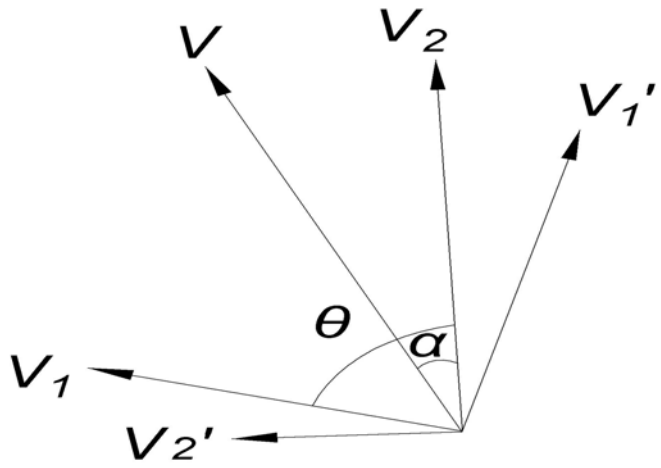

Fig. 2 Decomposition of velocity vector diagram

Considering the facts that the two adjacent stations are close; time interval of GW are very short and the radial velocity are estimated using the total echoes in each pixel, we assume the radial velocities at two adjacent stations are the two components of one vector(Fig. 2). This method has once been applied to retrieve the geostrophic velocity by altimetry data in the cross region:

$$V_1 = V \cdot \cos(\theta - \alpha) \quad , \tag{1}$$

$$V_2 = V \cdot \cos(\alpha) \, , \tag{2}$$

where V_1 and V_2 are the radial velocity at two adjacent stations; $V_1^{'}$ and $V_2^{'}$ are the tangential velocity; V is the vector velocity, θ is the angle between two point, α is the angle between V and V_2.

From Eqs. (1) and (2), the real velocity is

$$V = \frac{V_2}{\cos\left\{ arctg\left(\frac{V_1 - V_2 \cdot \cos\theta}{V_2 \cdot \sin\theta}\right)\right\}} \tag{3}$$

$$\alpha = arctg\left(\frac{V_1 - V_2 \cdot \cos\theta}{V_2 \cdot \sin\theta}\right) \tag{4}$$

2.2.2 Harmonic constants and tidal characteristics

We used the 'T_tide' toolbox to get the amplitude and phase of sub-tidal components(O_1, K_1, M_2 and S_2) at Luchao, Shengsi and Daishan tidal gauges. We derive the harmonic constants through analyzing the tidal velocity vectors. Following Chinese 'Code of Hydrology for sea harbor'[9], tidal characteristics are determined by $\lambda = (H_{O_1} + H_{K_1}) / H_{M_2}$, where H_{O1}, H_{K1}, H_{M2} are the major axis of elliptical tide for O_1, K_1, M_2. There are four types of tides on the basis of tidal characteristics: 1) $\lambda \le 0.5$, regular semidiurnal tide; 2) $0.5 < \lambda \le 2.0$, irregular semidiurnal tide; 3) $2.0 < \lambda \le 4.0$, irregular diurnal tide; 4) $4.0 < \lambda$, regular diurnal tide.

2.2.3 Tidal energy flux and tidal energy dissipation

Although GW radar measures sea surface velocity without the vertical structure of velocity, the study area is very shallow. We assume that the shallow ocean is one box, which means the velocity is uniform in each layer.

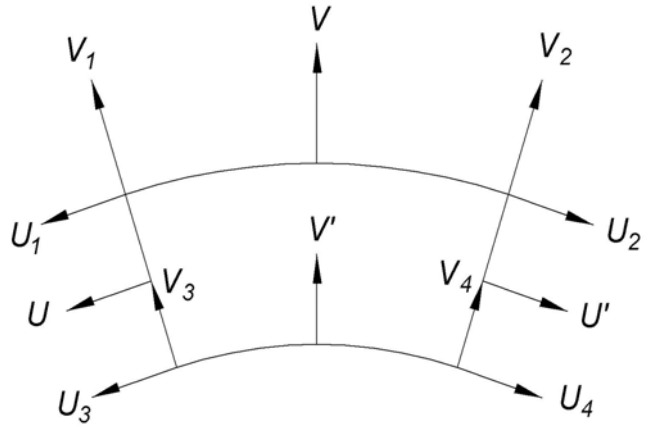

Fig. 3 Schematic of tidal energy flux algorithm

Fig. 3 shows the schematic of tidal energy flux algorithm. We use four stations to calculate the tidal energy flux. The radial velocity is $V=(V_1+V_2)/2$ and $V'=(V_3+V_4)/2$, and the tangential velocity is given by $U=(U_1+U_3)/2$ and $U'=(U_2+U_4)/2$. The lateral area is $S_{12}=(h_1+h_2)*\overline{12}/2$, where h_1 and h_2 is the water depth at station 1 and station 2, and $\overline{12}$ means the arc length between station 1 and station 2. The tidal energy is $E=0.5*V^2$, and then the tidal energy flux in each side is $\phi_e=V*S*E$. ϕ_e is positive(negative) when the water flow into(out of) the study area. The tidal energy dissipation is given by $\phi=\langle\phi_1+\phi_2+\phi_3+\phi_4\rangle$, where $\langle\ \rangle$ means time average.

Tab.1 Harmonic constants of three tidal stations

station	O_1		K_1		M_2		S_2		Characteristic value
	Amplitude / cm	Phase / °	Amplitude / cm	Phase / °	Amplitude / cm	Phase / °	Amplitude / cm	Phase / °	
Luchao	20.72	172	33.77	223	151.73	329	54.28	39	0.36
Shengsi	18.52	159	30.50	207	114.48	277	49.98	340	0.43
Daishan	20.51	171	31.90	222	104.87	296	41.06	358	0.49

3 Results

3.1 Velocity vectors

Fig. 4a shows the original radial velocity from GW radar. The westward velocity around 30˚42′N (-1.6 m/s) is a little larger than the surrounding velocities. Fig. 4b shows the retrieved velocity vectors. The water flows westward and converges into the bay. The velocity vectors are consistent with that under high tide condition in Hangzhou bay [10].

3.2 Harmonic analysis results

Four sub-tidal harmonic constants at each station are listed in Tab. 1. All of the tidal characteristics are between 0.28 - 0.47, which indicates that all over the stations are affected by the regular semidiurnal tides. The maximum major axis of ellipses is 1.28 cm (at station 11). The harmonic constants from tidal gauges also show that regular semidiurnal tides domain Luchao, Shengsi and Daishan stations (Tab. 2). Their tidal type is consistent with that from tidal gauge datasets [11].

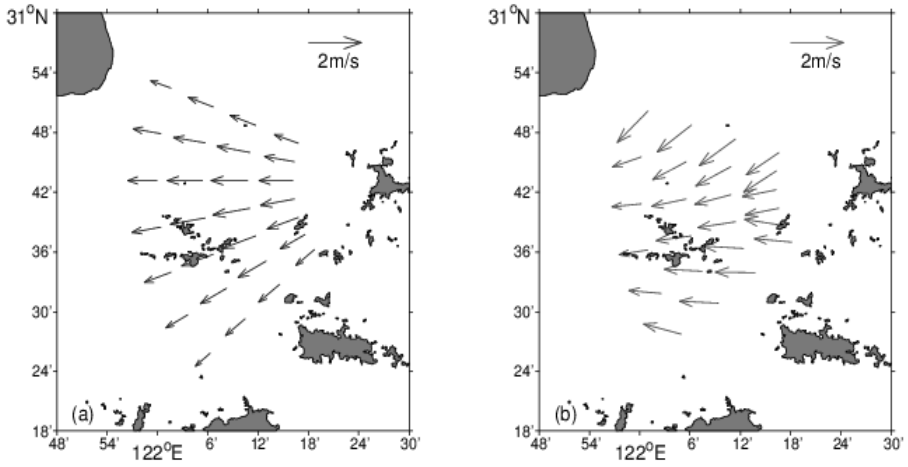

Fig. 4 Monthly averaged map of (a) the original radial velocity and (b)the retrieved flow vectors

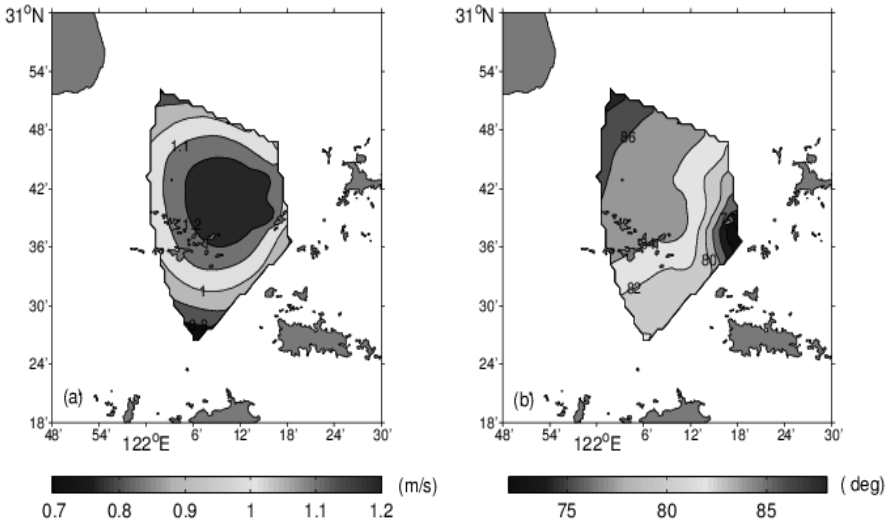

Fig. 5 Distributions of M_2 sub-tidal (a) velocity magnitude and (b) phase-field

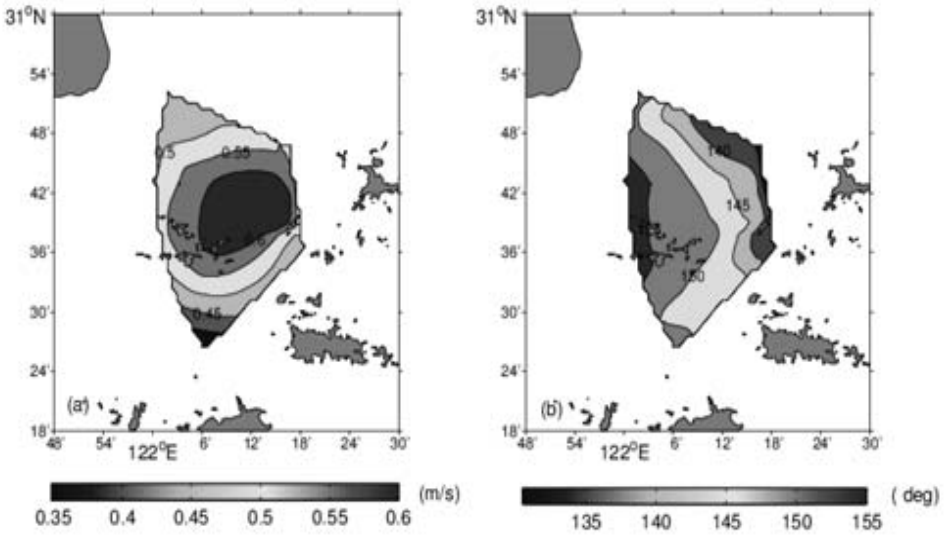

Fig. 6 Distributions of S2 sub-tidal (a) velocity magnitude and (b) phase-field

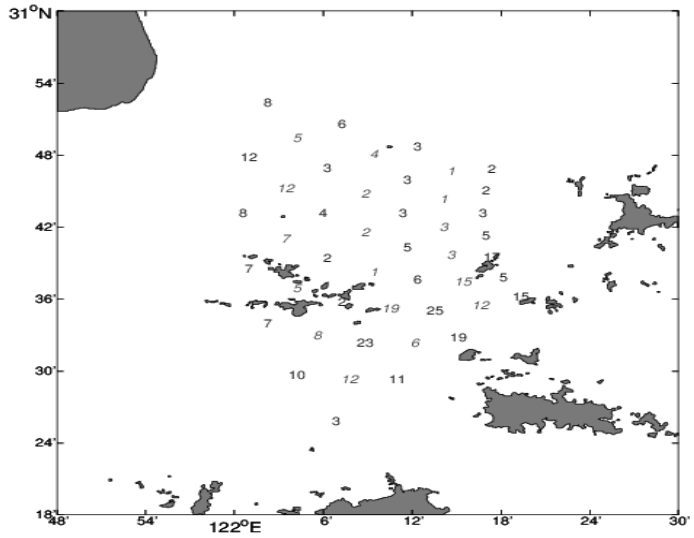

Fig. 7 Distributions of tidal energy dissipation rate(unit:104 m^3/s) (red number), and the water depth (blue number)

Since the semidiurnal tide domains the study area, we pay attention to the M_2 and S_2 sub-tidal components. Fig. 5a shows the sub-tidal velocity magnitude has a 'Sandwich' structure, which has maximum magnitude in the middle and minimum magnitude at the edge of the study area. It may result from the topography. When closer to the islands, the water depth becomes shallower and the velocity becomes smaller. The maximum velocity is 1.28cm/s. Fig.5b shows the M2 sub-tidal phase distributions. The higher phase in

northwest and lower phase in southeast indicate that the M_2 sub-tidal component flows into Hangzhou bay from southeast to northwest. Fig. 6a shows the S_2 sub-tidal velocity magnitude, which has the same pattern with M_2 sub-tidal component. The maximum velocity of S_2 is 0.63 cm/s. Fig. 6b is the S_2 sub-tidal phase distribution. The S_2 sub-tidal propagates westward from northeast.

Tab. 2 Harmonic constants of observation stations

station	O_1		K_1		M_2		S_2		Characteristic value
	Major axis/m	phase-lag/°	Major axis/m	phase-lag/°	Major axis/m	phase-lag/°	Major axis/m	phase-lag/°	
1	0.154 7	237	0.142 7	289	0.835 3	72	0.432 0	134	0.36
2	0.157 6	247	0.171 1	287	0.994 2	72	0.495 5	135	0.33
3	0.146 2	236	0.212 3	293	1.146 3	76	0.597 5	141	0.31
4	0.150 7	236	0.218 1	297	1.178 6	79	0.617 0	141	0.31
5	0.159 8	241	0.204 1	301	1.173 5	80	0.592 0	140	0.31
6	0.132 1	242	0.207 7	299	1.050 8	82	0.567 4	138	0.32
7	0.166 3	260	0.196 1	298	0.890 4	82	0.503 4	133	0.41
8	0.138 8	237	0.169 8	295	0.949 3	80	0.468 4	146	0.33
9	0.133 6	233	0.188 0	292	1.104 9	82	0.535 6	146	0.29
10	0.146 9	234	0.199 8	296	1.238 6	84	0.619 3	150	0.28
11	0.156 1	242	0.199 1	298	1.283 6	84	0.639 1	149	0.28
12	0.151 5	245	0.193 0	302	1.264 9	84	0.618 0	147	0.27
13	0.144 2	249	0.227 1	307	1.150 3	84	0.556 3	141	0.32
14	0.163 5	252	0.196 8	301	0.959 2	85	0.498 0	135	0.38
15	0.097 9	234	0.167 9	302	0.884 9	81	0.442 7	148	0.30
16	0.119 3	222	0.208 2	298	1.043 0	81	0.517 9	149	0.31
17	0.121 7	229	0.222 2	295	1.166 7	84	0.597 0	153	0.29
18	0.135 6	246	0.197 8	292	1.211 7	85	0.600 1	153	0.28
19	0.130 4	250	0.191 2	296	1.206 3	85	0.580 6	152	0.27
20	0.119 2	240	0.2054	307	1.102 7	85	0.510 9	149	0.29
21	0.108 5	242	0.207 4	294	0.911 8	87	0.467 1	142	0.35
22	0.156 9	217	0.071 9	291	0.669 5	83	0.334 6	152	0.34
23	0.152 4	233	0.100 3	282	0.858 9	81	0.428 7	150	0.29
24	0.165 4	238	0.143 4	277	0.972 8	84	0.495 3	156	0.32
25	0.171 5	231	0.147 8	288	1.004 5	86	0.528 4	157	0.32
26	0.152 4	239	0.162 8	284	1.016 5	87	0.493 6	159	0.31
27	0.101 9	248	0.224 1	305	0.959 2	87	0.476 6	153	0.34
28	0.147 6	210	0.203 7	299	0.746 7	90	0.451 6	156	0.47

3.3 Tidal energy dissipation

Fig. 7 shows the distribution of water depth and the tidal energy dissipation. The blue

numbers are the water depths and the red one are the tidal energy dissipation rates, with unit 104 m^3/s. We found the maximum tidal energy dissipation rate is 19×104 m^3/s. The smaller gradient of water depth corresponds to the smaller tidal energy dissipation rate. It indicates that the tidal energy dissipation is related to the topography.

4 Discussion and conclusions

1）We retrieve the velocity vector based on single-point GW radar radial velocity. We also compare the four sub-tidal components(O_1,K_1,S_2,M_2) from the velocity vectors with that from the tidal gauge datasets using harmonic analysis. The two datasets show the same tidal characteristics and tidal types in our study area. It indicates that the retrieved velocity vector from single-point GW radar is convincible and feasible to investigate the tidal information.

2）We assume the velocity in each layer is the same with the surface velocity. It ignores the velocity shear, but it could reflect the tidal characteristics in small scale. To get much higher accuracy, vertical structure of velocity is needed.

3）The tidal energy dissipation rate from GW radar agrees well with the gradient of water depth. In the steep continental shelf, the tidal energy dissipation rates are large; while in smooth region, the tidal energy rates are small.

Acknowledgments

This work was supported by projects (No. 40976012 and No. 40906030). We thank Professor WEN Bi-yang from WuHan University for providing the ground radar observation data.

References

[1] Ke Heng-yu, Wu Shi-cai, Yang Zi-jie, et al. Application of HF Ground Wave Radar to EEZ [J]. Journal of University of Wuhan Iron and Steel Corporation, 1999, 11(2): 23 - 30.

[2] Zhou Zhi-xin, Liu Yong-tan. Computational Method for the Extraction of Suface-Current by HF Ground-Wave-Radar [J]. Marine Science Bulletin, 1997, 16(5): 79 - 84.

[3] ZHOU Hao, WEN Bi-yang, LIU Hai-wen. Ocean Surface Vector Current Synthesization of HF Ground Wave Radar [J]. Wuhan University Journal(Natural Science Edition), 2001, 47(5): 642 - 644.

[4] ZHU Da-yong, SHAO Hao, LI Yan, et al. Quality analyses of radial currents measured by a

demonstration system of OSMAR HF radar in Fujian Province [J]. Journal of Oceanography in Taiwan Strait, 2007, 26(1): 8 - 16.

[5] Mackinnnon J A, Gregg M C. Shear and baroclinic energy flux on the summer New England shelf [J]. J. Phys. Oceanogr., 2003, 33: 1 462 - 1 475.

[6] Nash J D, Kunze E, Toole J M, et al. Internal tide reflection and turbulent mixing on the continental slope [J]. J. Phys. Oceanogr., 2004, 34:1 117 -1 134.

[7] ZHANG Xiao-qian, LIANG Xin-feng, ZHOU Lei. Estimates of M2 internal tide energy fluxes in the Pacific Ocean using TOPEX/Poseidon altimeter data [J]. Acta Oceanologica Sinica, 2005, 27(5): 9 - 14.

[8] LI Pei-Liang, LI Lei, ZUO Jun-Cheng, et al. Tidal Energy Fluxes and Dissipation in the Bohai Sea, the Yellow Sea and the East China Sea [J]. Journal of Ocean University of Qingdao, 2005, 35(5): 713 - 718.

[9] The ministry of communications of the People's Republic of China. JTJ213-98, Code for sea port hydrology. Beijing: people's traffic press, 1998.

[10] Li Shenduo, Hu Hui. A study on the current fieled of the HangZhou bay [J]. Oceanologia Et Limnologia Sinica. 1987, 18(1): 28 - 37.

[11] Chen Qian, Huang Da-ji, Zhang Ben-zhao, et al. Characteristics of the tidal current and residual current in the seas adjacent to Zhejiang [J]. Donghai Marine Science, 2003, 21(4): 1 - 14.

单点高频地波雷达资料估算潮能耗散的方法

毛华斌，陈 举，邱春华，练树民

（中国科学院南海海洋研究所 热带海洋环境国家重点实验室，广东 广州 510301）

摘 要：使用崾泗站所布设的地波雷达观测获取的径向流数据，以及崾泗、芦潮港、岱山3个潮汐观测站水位资料，采用两点近似投影方法反演流场全矢量流速，并用T_tide程序计算调和常数，分别计算O_1、K_1、M_2、S_2各分潮流速场及迟角场，并计算各点上的潮能通量及潮能耗散，得到崾泗岛以西杭州湾口区域潮能耗散同地形存在良好对应关系，充分证明了采用地波雷达观测数据进行潮能耗散计算这一方法的可行性，供相关工作者作进一步研究和讨论。

关键词：地波雷达；特征值；潮汐类型；潮能通量；潮能耗散